Accurate binding of sodium and calcium to phospholipid bilayers by effective inclusion of electronic polarization

Josef Melcr and Hector Martinez-Seara Monne

Institute of Organic Chemistry and Biochemistry, Academy of Sciences of the Czech Republic, Prague 6, Czech Republic

Jiří Kolafa

Department of Physical Chemistry, Institute of Chemical Technology, Prague 6, Czech Republic

Pavel Jungwirth

Institute of Organic Chemistry and Biochemistry, Academy of Sciences of the Czech Republic, Prague 6, Czech Republic and
Department of Physics, Tampere University of Technology, P.O. Box 692, FI-33101 Tampere, Finland

O. H. Samuli Ollila*

Institute of Organic Chemistry and Biochemistry, Academy of Sciences of the Czech Republic, Prague 6, Czech Republic and
Institute of Biotechnology, University of Helsinki

(Dated: October 22, 2017)

Despite of the significant biological relevance, the binding details of cations in cellular lipid membranes are not fully understood. For example, consistent results for the binding affinities and stoichimetries of Na^+ and Ca^{2+} ions to phospholipid bilayers have not been achieved with different experimental and theoretical methods. The ion binding details could be resolved with classical molecular dynamics (MD) simulations, however, the accuracy of the available lipid models has not been sufficient. In this work we show that the binding details of Na^+ and Ca^{2+} ions to 1-Palmitoyl-2-oleoylphosphatidylcholine (POPC) bilayer can be accurately described with a MD simulation model having implicitly included electronic polarization. This is demonstrated by applying the electronic continuum correction (ECC) to a state of the art lipid model for MD simulations of POPC lipid bilayer. The introduced ECC-lipid model reproduces the experimentally measured structural parameters for the ion-free membrane, the response of lipid headgroup to the bound positive charge, and the binding affinities of Na^+ and Ca^{2+} ions. The imperceptible binding of Na^+ ions to POPC bilayer and interactions of Ca^{2+} mainly with phoshpate oxygens in the ECC-lipid model give support to the early intepretations of the experimental spectroscopic data. On the other hand, Ca^{2+} ions form complexes with 1-3 lipid molecules with almost equal probabilities, suggesting more complicated binding stoichimetry than the ternary complex binding model used to interpret the NMR data. The results in this work pave the way for MD simulations of complex biochemical systems with realistic electrostatic interactions in the vicinity of cellular membranes.

I. INTRODUCTION

Cation interactions with cellular membranes play a key role in several biological processes, such as signal propagation in neurons and vesicle fusion. Since the direct measurements of ion-membrane interactions from biological systems are difficult, lipid bilayers are often used as models systems for cellular membranes. Especially the zwitterionic phosphocholine (PC) lipid bilayers are used to understand the role of ions in complex biological systems [1–3].

Interactions of biological cations, especially Na^+ and Ca^{2+}, with PC bilayers are widely studied in experiments [2–9] and classical MD simulations [10–14]. The details of ion binding are, however, not fully consistent in the literature. Interpretations of non-invansive spectroscopic methods, like nuclear magnetic resonance (NMR), scattering and infrared spectroscopy suggest that Na^+ ions exhibit negligible binding to PC lipid bilayers with submolar concentrations, while Ca^{2+} specifically binds to phosphate groups of two lipid molecules [4, 5, 7–9, 15–17]. Atomistic resolution molecu-lar dynamics (MD) simulation models, however, predict significantly stronger binding for the cations than NMR experiments [18]. On the other hand, some experiments have also been interpreted to support the predictions from MD simulations [10, 19]. Furthermore, interactions of Calcium ions with 3-4 lipids, including also interactions with carbonyl oxygens, have been reported from simulations [10, 11, 13, 14].

Recent work published by the NMRlipids project (nmrlipids.blogspot.fi) [18] made an attempt to resolve the apparent controversies. A direct comparison of ion binding affinities to PC bilayers was presented between simulations and experiments by using the electrometer concept, which is based on the experimental NMR data for the lipid headgroup order parameters [20]. Using massive amounts of data collected by Open Collaboration method, it was concluded that the accuracy of the current state of the art lipid models for MD simulations is not sufficient for the detailed interpretation of the cation interactions with PC lipid bilayers [18].

In this work we show that the cation binding behavior in MD simulations of 1-Palmitoyl-2-oleoylphosphatidylcholine (POPC) bilayer can be significantly improved by implicitly including the electronic polarizability in the polar region of lipid molecules. The electronic polarizability is included by using

*samuli.ollila@helsinki.fi

the electronic continuum correction (ECC) [21], which has been previously shown to improve the behaviour of MD simulations of ions in bulk water [22**?** –24]. As a starting point we use the parameters from the Lipid14 model [25], which gave the best cation binding behaviour in the previous study [18]. The developed ECC-lipid parameters reproduce the experimentally measurable structural parameters of an ion-free POPC lipid bilayer with the accuracy comparable to the other state of the art lipid models, while surpassing them significantly for reproducing the membrane binding affinities and induced structural effects of Sodium and Calcium ions.

II. METHODS

A. Electronic continuum correction for lipid bilayers

The lack of electronic polarizability in the standard MD simulation force fields has been considered a higly relevant issue since the early days of lipid bilayer simulations. In this work we circumvent the rather demanding explicit inclusion of electronic polarization effects [26, 27] by implicitly including electronic polarizability in lipid bilayer simulations by using the electronic continuum correction (ECC) [21]. Technically, it is a similar approach to the phenomenological charge-scaling as applied in earlier studies [28, 29]. **1.We should also cite papers where empirical scaling was used ionic liquids DOI: 10.1002/anie.201308760** The present concept of ECC is, however, physically well justified and rigorously derived [21, 30, 31].

Following the ECC concept, electronic polarizability can be effectively included in classical MD simulations by placing all particles into a homogeneous dielectric continuum with a dielectric constant ϵ_{el}, which is the electronic part of the dielectric constant of the media [21]. Following the Coulomb's law, such a dielectric continuum can be easily included in standard MD simulation by a scaling of charges

$$Q^{ECC} = f_q \cdot Q \qquad (1)$$

with a constant scaling factor $f_q = \epsilon_{el}^{-1/2}$ effectively representing the newly introduced electronic continuum. Given the high frequency dielectric constant as measured in water (corresponding to the square of the refraction index) of $\epsilon_{el} = 1.78$, the scaling factor for aqueous ions is $f_q = 0.75$ [21**?**]. This scaling factor has been successfully used to improve the performance of force field for ions in solution [23**?** , 24], which then agree quantitatively with neutron scattering data [22–24].

While the scaling factor of $f_q = 0.75$ for ions in water improves their description and is physically well justified within the ECC theory [**?**], it is not a priori clear whether the same factor should be used for partial charges in molecules, e.g., lipids in our case. Unlike the total charge of an atom or molecules, atomic partial charges within molecules are not physical observables. There are thus several schemes for the assignment of partial charges for biomolecules [32]. Currently, the most commonly employed scheme is the restrained electrostatic potential (RESP) method [33, 34]. By construction, partial charges currently implemented in force fields may

already include to some extend the solvent electronic polarizability effects, i.e., the RESP charges are often scaled to fit certain experimental observables **2.This needs a citation - Joe please pick 1-2 papers**. Thus, a consistent application of the ECC scaling factor, f_q, to the molecular partial charges included in the available force fields does not necessarily have to follow the above relation $f_q = \epsilon_{el}^{-1/2}$, but instead it lies between 0.75 i.e., (no electronic polarizability included in the original partial charges) and 1 (i.e., electronic polarizability fully included in the original partial charges). It is important to note that even thought the lipid bilayer interface has a large gradient in the total dielectric constant, the electronic polarizability part can be considered to be constant as the measurements of high frequency dielectric constant gives values around 2 for almost any biologically relevant material [21**?**].

In this work, we employ the ECC to develop a classical MD simulation model for a POPC lipid that accurately describes the binding of Sodium and Calcium ions to a lipid bilayer. The model quality in terms of the ion binding is measured by directly comparing simulations to the experimental NMR data used to measure the ion binding affinity [4, 5, 35], as discussed in detail in Ref. 18. The Lipid14 [25] force field parameters (available in Gromacs format from Ref. 36) were used as a starting point, because they give the most realistic response to the bound ions and to the NaCl concentration among the available lipid models (see Figs. 5 and 2 in Ref. 18). Moreover, the Lipid14 model gave relatively realistic glycerol backbone and head group structures when compared with the other state of the art lipid models [37].

The ECC correction was applied to the Lipid14 parameters by scaling partial charges of the head group, glycerol backbone, and carbonyl regions, which are the most polar parts in the lipids and are thus expected to have the largest contribution to the cation binding. We do not modify the hydrocarbon chain parameters, as they do not come in direct contact with salt ions and are already highly optimized to provide a good description for the hydrophobic part of lipid bilayers [25, 38]. This is in contrasts with the glycerol backbone and the head group regions, which call for improvements in all available lipid models [37].

The values within the above discussed parameter space for the scaling factor, $f_q \in (0.75, 1.0)$, were explored to find the optimal value to reproduce the experimental ion binding affinity. We observed that the scaling of the partial charges reduced the ion binding affinity and the related head group order parameter response in general. By comparing the results with different scaling factors to the experimental NMR data [4, 5, 35] we found the optimal value of $f_q = 0.8$, which is only slighly higher than the scaling factor for the ions in water 0.75.

While, the scaling of the partial charges improved the ion binding affinity, it reduced the bilayer area per lipid below the experimental value. After scaling the partial charges of the head group, the glycerol backbone and carbonyls with a factor of 0.8, the simulation gave the approximately 60 Å^2 for the area per lipid, which is somewhat smaller than the experimental value, 64.3 Å^2 [39], as well as the value given by the original Lipid14 parameters, 65.6 ± 0.5 Å^2 [25]. The decrease

of the area per lipid is found to arise from a reduced hydration of the lipid head group region, due to the lower polarity of molecules with scaled charges. This can be compensated by reducing the effective radius of atoms with the scaled charges by changing the σ parameters in the Lennard-Jones potential, as previously done for ions in solution [22–24]. After reducing these σ parameters by a factor of $f_\sigma = 0.89$, the area per molecule is restored back close to the experimental value (see Table I).

3.We should discuss how this can potentially affect the intermolecular interaction when mixing scaled and non scaled molecules.

JOE: I think that we rather increasingly see that there's nothing like "fully non-scaled" with the exception of ions with integer charges. So the discussion shall be rather more about the interaction of our "scaled" (I'd still rather call it ECC-corrected or whatever) and "semi-scaled" models.

SAMULI: There is now a paragraph in the conclusions, which mentions this topic.

B. Electrometer concept

Ion binding in lipid bilayers was compared between experiments and simulations by using the lipid head group order parameters and the "electrometer concept" [18, 20], which is based on the experimental observation that the C-H bond order parameters of α and β carbons in PC lipid head group (see Fig. 1) are proportional to the amount of charge bound per lipid [20]. The change of order parameters measured with varying aqueous ion concentration can be then related to the amount of bound ions.

The concept can be used to compare the ion binding affinity to lipid bilayers between MD simulations and NMR experiments, because the order parameters can be accurately determined from both techniques [18, 38]. The order parameters for all C-H bonds in lipid molecules, including α and β segments in head group, can be accurately measured using ^{2}H NMR or ^{13}C NMR techniques [38]. From MD simulations the order parameters can be calculated using the definition

$$S_{\mathrm{CH}} = \frac{3}{2}\langle\cos^2\theta - 1\rangle, \qquad (2)$$

where θ is the angle between the bond and membrane normal and the average is taken over all sampled configurations [38].

The relation between the amount of the bound charge per lipid, $X^\pm$, and the head group order parameter change, ΔS_{CH}^i, is empirically quantified as [20, 40]

$$\Delta S_{\mathrm{CH}}^i = S_{\mathrm{CH}}^i(X^\pm) - S_{\mathrm{CH}}^i(0) \approx \frac{4m_i}{3\chi}X^\pm, \qquad (3)$$

where $S_{\mathrm{CH}}^i(0)$ denote the order parameter in the absence of bound charge, i refers to either α or β carbon, m_i is an empirical constant depending on the valency and position of the bound charge, and the experimental value [41, 42], $\chi \approx 167\,\mathrm{kHz}$, is used for the quadrupole coupling constant. Atomic absorption spectra and ^{2}H NMR data gave $m_\alpha = -20.5\,\mathrm{kHz}$ and $m_\beta = -10.0\,\mathrm{kHz}$ for the binding of Ca^{2+} to POPC bilayer (in the presence of 100 mM NaCl) [5, 18, 38]. The slopes are negative, because the head group order param-

eters decrease with bound positive charge and increase with bound negative charge [18, 38]. This can be rationalized as a change of the lipid head group dipole tilt toward water phase with the bound positive charge and *vice versa* with the negative charge [20].

The measured order parameter change depends on both, the head group response to the bound charge and the amount of bound charge, i.e. m_i and $X^\pm$ in Eq. 3, respectively. The former property has to be well quantified before the electrometer concept can used to analyze the binding affinities, as done experimentally for a wide range of systems [20, 43]. To calibrate the head group order parameter response to the bound charge in simulations, we use the experimental data for dihexadecyldimethylammoniumbromide mixed within a POPC bilayer [35]. Dihexadecyldimethylammonium
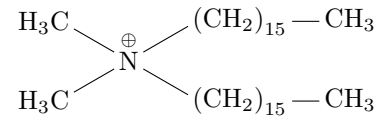
is a cation surfactant having two acyl chains and bearing a unit charge in the hydrophilic end. Thus, it is expected to locate in the bilayer similarly to the phospholipids and the molar ratio then gives directly the amount of bound unit charge per lipid $X^\pm$ in these systems [35].

C. Salt concentrations and binding affinity

The early electrometer concept data for the lipid head group order parameter changes from the NMR experiments was reported as a function of the salt concentration in water before solvating the lipids [4]. The later study used also the atomic absorption spectroscopy and reported the order parameter changes as a function of the salt concentration in the supernatant after the solvation of lipids [5]. In this work we focus on POPC for which the latter definition was used [5]. The salt concentration in the aqueous bulk region was calculated from the farthest point from both lipid leaflets in the water phase. Note that in the previous study, Ref. 18, the ion concentrations were calculated in water before solvating the lipids as in the earlier experiments [4]. Despite of the measurable differences between these two definitions of concentrations for CaCl$_2$ systems, the qualitative conclusions in this or in the previous work [18] are not affected by this.

To quantify the ion binding affinity to a lipid bilayer, we calculated the relative surface excess of ions with respect to water, Γ_i^w [44]. This quantity was chosen because it does not depend on the position of the Gibbs dividing plane between two bulk regions. Here we assume that the interface locates between the hydrophobic interior of a lipid bilayer and the bulk water region far from the membrane. The bulk concentration of ions and water is zero inside the bilayer. The concentrations in bulk water region can be calculated from the farthest point from both lipid leaflets in the water phase. The region between these boundaries contains all the ions and water molecules in the simulation box. This setup provides a

simplified relation for Γ_i^w in lipid bilayers simulations

$$\Gamma_i^w = \frac{1}{2A_b}\left(n_i - n_w\frac{C_i}{C_w}\right), \quad (4)$$

where n_w and n_i are the total number of waters and ions in the system; C_w and C_i are their respective bulk concentrations in the aqueous phase; and A_b is the area of the box in the membrane plane. The total area of the interface is twice the area of the membrane, $2A_b$, because bilayers have an interface at both leaflets.

D. Validation of lipid bilayer structure against experiments

The structure of lipid bilayers in simulations without ions were validated against NMR and x-ray scattering experiments by calculating the order parameters for C-H bonds and the scattering form factors. The former validates the structures sampled by the individual lipid molecules in simulations with atomic resolution, while the latter validates the dimensions of the lipid bilayer (thickness and area per molecule) [38].

The order parameters were calculated from simulations for all C-H bonds in lipid molecules by using Eq. 2. Form factors were calculated from equation **4.As Hector suggested, it might be better to write the simpler form for this equation.**

$$F(q) = \int_{-D/2}^{D/2}\left(\sum_\alpha f_\alpha(q_z)n_\alpha(z) - \rho_s\right)\exp(izq_z)\mathrm{d}z, \quad (5)$$

where $f_\alpha(q_z)$ is the density of atomic scattering length, ρ_s is the density of solvent scattering length in the bulk region, $n_\alpha(z)$ is the number density of atom α and z is the distance from the membrane centre along its normal spanning until the water bulk region, D.

E. Simulation details

1. Simulations of POPC bilayers with aqueous ions

Simulations of POPC bilayer in pure water or in varying salt concentrations contained 128 POPC molecules and approximately 50 SPC/E water [45] molecules per each lipid in the periodic orthorhombic simulation box. The chosen water model has the optimal dielectric constant to be used with the ECC modified molecules **5.Citation or discussion.** and it has been was also used in the previous parametrization of ECC ions [22, 24**?**]. The results with other water models are available in SI. The ECC-ion models **6.Specify the exact version.** were used for Sodium, Calcium and Chloride ions [22, 24**?**]. Simulation with the Lipid14 model was also ran with the ion model by Dang et al. [46–48]**7.Which water model was used in this simulation?.** Simulation data for the Lipid14 model with Åqvist [49] ion and TIP3P [50] water models are reported in [18] and were taken directly from [51–54]. MD simulations were performed using the GROMACS [55] simulation package (version 5.1.4). The simulation settings used in this work are summarized in

TABLE I: Area per lipid (APL) values of POPC bilayer without ions from the Lipid14 simulation ran in this work and from the literature, from the ECC-lipid model and from experiments.

model	APL (Å^2)	Temperature [K]
Lipid14	65.1 ± 0.6	300
Lipid14 [25]	65.6 ± 0.5	303
ECC-lipids	62.2 ± 0.6	300
experiment [39]	64.3	303

Table IV. Simulation trajectories and parameters are available at [**?**] **8.To be uploaded to Zenodo.**

2. Simulations of POPC bilayers with cationic surfactants

An automated topology builder [56] was first used to create the structure of dihexadecyldimethylammonium. The AmberTools program [57] was then used to generate the Amber-type force field parameters. The parameters were converted to the Gromacs format by using the acpype tool [58]. The partial charges were then manually modified to approximately correspond to their equivalent segments in Lipid14 [25]. The parameters together with the simulation data are available at [59–64]. The surfactants were randomly placed among the lipids to form bilayer structures with mole fractions of 10%, 20%, 30%, 42%, or 50% of surfactant in the POPC bilayer. All systems contained 50 POPC molecules per leaflet, 6340 TIP3P [50] water molecules and 6, 14, 21, 35, or 50 surfactants per leaflet. Chloride counter ions were used in simulations, because parameters for bromide, the counterion in the experimental data [35], were not available in the standard Gromacs files for Amber force field. The Lipid14 model was used for POPC. The first 20 ns of the total simulation time of 200 ns was considered as an equlibration time and was omitted from the analysis. A reasonable lipid neighbor exchange occured during the simulation.

The same systems were also simulated with the ECC-lipid model for POPC using the same setup. **9.Which water model was used in these simulations?** In these simulations the ECC correction was also applied to the cationic surfactant by scaling all charges with the same factor as for ECC-lipids, i.e., $f_q = 0.8$, and by using the atom types with reduced σ parameters from ECC-lipids. **10.Parameters are available at ??**

III. RESULTS AND DISCUSSION

A. POPC membrane structure and dynamics

The ECC-lipid and Lipid14 models reproduce the experimental x-ray scattering form factors of POPC bilayer with the similar accuracy in Fig. 1. The area per lipid values from the Lipid14 model is slightly larger than the experimental value in Table I, while the value from ECC-lipid model is slightly smaller. Area per lipid values of the ECC-lipid model show
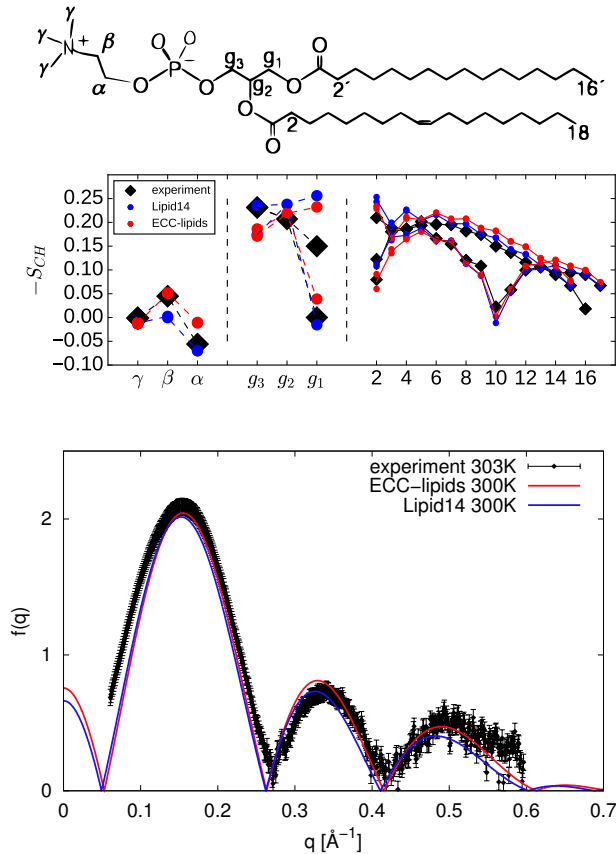
FIG. 1: Top: The chemical structure of POPC and the labeling of the carbon segments. Middle: Order parameters of POPC head group, glycerol backbone and acyl chains from simulations with the Lipid14 [25] and the ECC-lipid models compared with the experimental values from [65]. The size of the points for the head group order parameters correspond the error bars (± 0.02 for experiments [37, 38] and ?? for simulations **Add the size of the error bars in simulations.**). The size of the points for acyl chains are decreased by a factor of 3 to improve the clarity of the plot. Bottom: X-ray scattering form factors from simulations with the Lipid14 [25] and the ECC-lipid models compared with experiments [**?**].

11.Increase the height of the order parameter figure

12.sn-1 and sn-2 order parameters should be somehow labelled in the order parameter figure. Maybe empty and filled points?

13.Would it be possible to increase the size of points for acyl chain order parameters only in z-direction such that it would correspond the error bars?

14.x-axis in form factor plot from 0 to 0.6, where experimental data ends. y-axis from 0 to ~2.2 to remove the empty space.

some variation when simulated with different water models in Table III (Supplementary Information), however, all the values are close to the experimentally reported values. In conclusion, the ECC-lipid model reproduces the experimental dimensions of POPC lipid bilayer with the accuracy comparable to the other state of the art lipid models [38].

The acyl chain order parameters of the Lipid14 model [25] and the ECC-lipid model agree with the experimental values with in the error bars in Fig. 1, although the ECC-lipid model gives slightly larger values for *sn*-1 chain. Notably, the exper-

imentally measured forking and small order parameter values of C_2 segment in *sn*-2 chain are relatively well reproduced by the both models. This has been suggested to indicate that the carbonyl of *sn*-2 chain is directed towards the water phase, in contrast to the carbonyl in *sn*-1 chain, which would orient more along the bilayer plane [66–68]. While this may be an important feature for the ion binding details, it is not necessarily reproduced by the available lipid models [38]

The order parameters of α and β carbons in the headgroup are slightly larger in the ECC-lipid model than in the Lipid14 model, which is apparently related to the P-N vector orienting $7°$ more toward the water phase in the ECC-lipid model, see Fig. 2. With the current data we cannot, however, conclude which one of the models give the more realistic headgroup conformations. The ECC-lipid model gives the β carbon order parameter value closer to experiments, while value for α carbon is better in the Lipid14 model. Despite of some deviations from the experimental order parameter values in Fig. 1, the accuracy of the both models in the glycerol backbone region is comparable to the other state of art lipid models available in literature [37].

15.Dynamics check is missing: MSD (Hector/Joe)

B. Calibration of lipid electrometer: Response of POPC head groups to bound charge

Before proceeding to the ion binding affinity, we quantify the response of the headgroup order parameters to the amount of bound charge by using mixtures of monovalent cationic surfactants (dihexadecyldimethylammonium) and POPC [35]. The amount of bound charge per PC in these systems is given by the molar fraction of cationic surfactants, because essentially all surfactants with two hydrophopic acyl chains can be assumed to locate in the lipid bilayers. The experimental data for these systems can be used to validate the sensitivity of lipid headgroup order parameters to the amount of bound charge in simulations.

The changes of the headgroup order parameters with an increasing amount of the cationic surfactant is compared between experiments [35] and simulations in Fig. 2. Approximately linear decrease of the order parameters, as expected from Eq. 3, is observed in simulations and experiments at least for the mole fractions below $\sim 30\%$. The slope is, however, too steep in the Lipid14 model indicating that the head group order parameters respond too sensitively to the bound positive charge. The slope in the ECC-lipid model is in very good agreement with experiments for the α segment, while the slope is slightly underestimated for the β segment.

The headgroup P-N vector angle with respect to the membrane normal is also shown in Fig. 2 as a function of the mole fraction of the cationic surfactant. As suggested previously [20], the headgroup orients more towards the water phase with the increasing amount of positive charge in a PC lipid bilayer. The effect is more pronounced in the Lipid14 model, for which the addition of 50% mole fraction of the cationic surfactant leads to the decrease of $20°$ of the P-N vector angle, while the corresponding change in the ECC-lipid
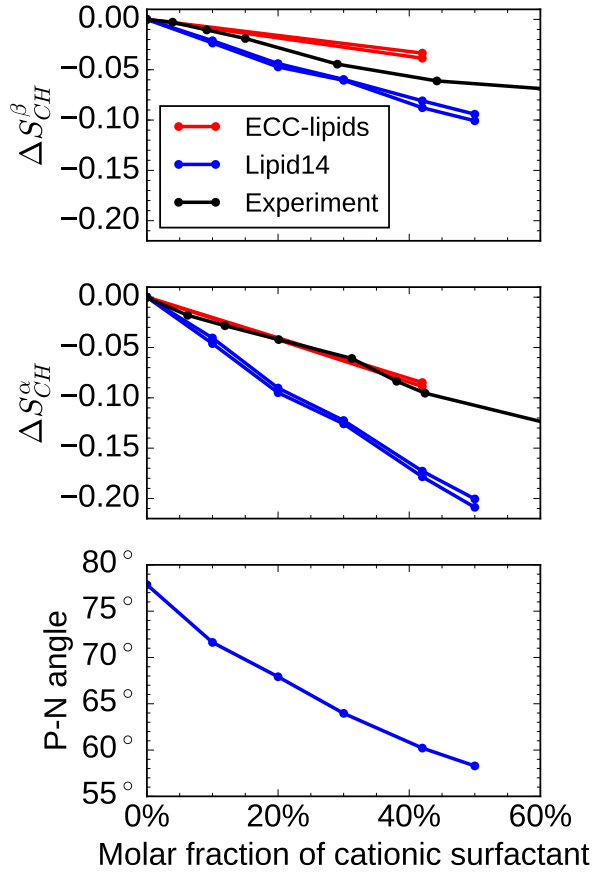
FIG. 2: The changes of headgroup order parameters and P-N vector orientation as a function of cationic surfactant (dihexadecyldimethyl-lammonium) in POPC bilayer from simulations and experiments [35].

16.Labeling should be consistent with the previous figure, i.e. experimental data with diamonds.

17.x-axis scale from -1 to 51 to make the point in zero fully visible and to remove empty space.

18.Empty space between figures and from the right column could be reduced.

19.Put the experimental data with larger points and thicker line in this and in the next two figures to make more clear separation between simulation and experimental data.

model is $11°$. The difference is in line with the smaller order parameter changes and the reduced charge–dipole interactions in the latter model. The lesser sensitivity of the P-N vector angle response in the ECC-lipid model can be considered to be more realistic, because the changes of the headgroup order parameters as a function of the bound positive charge are in better agreement with experiments in this model. The results also imply that the validation and improvements of MD simulation models are generally required for the reliable simulation studies of the lipid headgroup responses to ions or other biomolecules, as also concluded previously [37].

C. Binding affinities to POPC membrane validated through lipid electrometer

The changes of the lipid bilayer headgroup order parameter from different simulations and experiments [4, 5] are shown in Figs. 3 and 4 as a function of NaCl and $CaCl_2$ concentrations. These results can be used to compare the ion binding affinities to lipid bilayers between simulations and experiments by using the electrometer concept, because the order parameters decrease proportionally to the amount of bound positive charge [18, 20]. The recent comparison of different simulation models to the experimental data revealed that most models significantly overestimate the Na^+ ion binding to PC lipid bilayers and that none of the available models correctly reproduce the details of the binding of Ca^{2+} ions [18]. A positive exception was the Lipid14 model [25] simulated with Åqvist ions, as seen from the data replotted from Ref. 18 in Figs. 3 and 4. The model reproduced the experimentally measured small order parameter changes with NaCl and imperceptible Na^+ binding to PC bilayers [4, 5]. However, the changes of the headgroup order parameters as a function of $CaCl_2$ concentration were overestimated by the same combination of force field parameters.

Since significant artefacts are reported in simulations with Åqvist ions is water [**?**] **30.Add citations**, we also simulated the Lipid14 model with the ion models by Dang et al. [46–48] and ECC-ions [22, 24**?**] having more realistic bulk behaviour. Instead of the improvement in the binding behaviour, we observed overbinding also of Na^+ with these ions models, while the results with Ca^{2+} were barely affected, as seen in Figs. 3 and S**??**.**31.Add OP-response of Lipid14+ECC-ions plot in SI**. The results are in line with the previous work [18], suggesting that the improvements in the lipid parameters are required to correctly describe the divalent cation binding to PC lipid bilayers.

The results from the simulations with the ECC-lipid and the ECC-ion models [22, 24**?**] exhibit an improved behaviour of cation binding to a POPC bilayer in Fig. 3, showing a good agreement with experiments in the changes of the lipid headgroup order parameters as a function of NaCl and $CaCl_2$ concentrations. Since also the headgroup order parameter response the to the bound positive charge the ECC-lipid model was in good agreement with experiments in section III B, we conclude that the model correctly reproduces the binding affinity of Na^+ and Ca^{2+} ions to POPC lipid bilayer. Also the response of the glycerol backbone g_3 order parameter to $CaCl_2$ was significantly overestimated in the original Lipid14 model, while the ECC-lipid gives a good agreement with exepriments, as seen in Fig. 3. Also the changes of the P-N vector angle are more pronounced for the Lipid14 model, for which the maximum $CaCl_2$ induced tilting toward water phase is approximately $17°$, while the corresponding value for ECC-lipid model is $6°$.

Furthermore, the overestimated lipid headgroup order parameter changes of POPC in the Lipid14 model as a function of $CaCl_2$ concentration arise from both, the overestimated binding affinity and sensitivity of the headgroup tilt to the bound positive charge. This probably applies also to the other lipid models considered in the previous study [18], emphasiz-
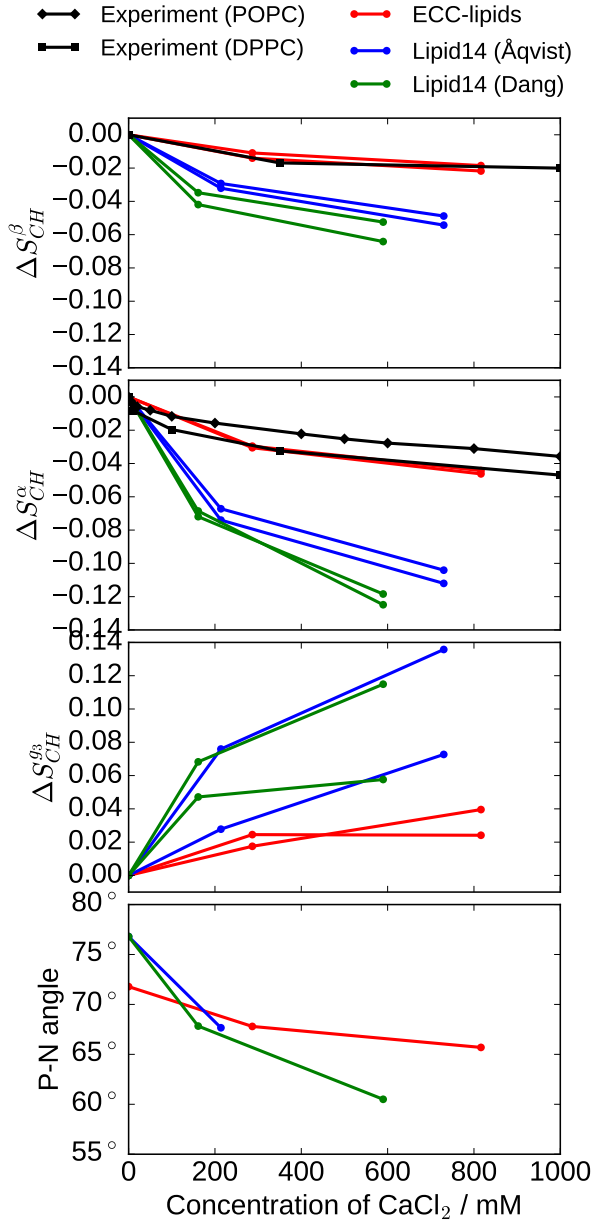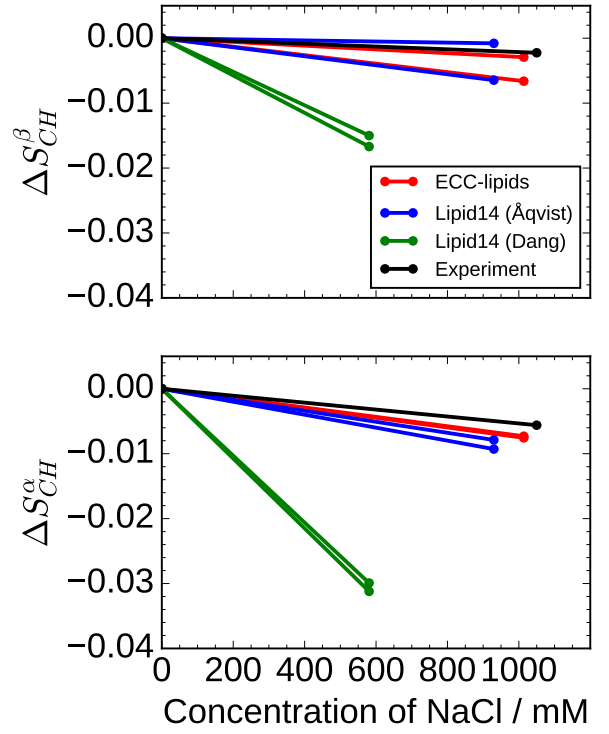
FIG. 3: The changes of the head group order parameters of POPC bilayer as a function of CaCl$_2$ concentrations are shown from simulations with different force fields together with experimental data (DPPC [4] and POPC [5]). Ion concentrations in bulk water are shown in x-axis. Values from simulations are calculated from the of cation number density C_{np} from the region at the simulatin box edge with the constant ion concentration as [ion]=C_{np}/0.602. Simulation data with Lipid14 and Åqvist ion parameters are taken directly from Refs. [51–53].

20.Maybe experimental points and lines could be larger to make a more clear differentce to simulations

21.Add temperatures for POPC and DPPC experiments

22.y-axis scale of the bottom figure from 59 to 78 to remove the empty space.

23.Empty space from the right column could be reduced.

24.Experimental values from [4] to be put in the g_3 figure: the value of g_3 order parameter of DPPC was -0.214 in the absence of ions [average of two closely spaced splittings] and -0.211 in the presence of 0.35 M CaCl$_2$ (at 59 Celcius). No effect of ions could be detected on DPPC bilayers labeled at the C-2 segments of both fatty acyl chains."

FIG. 4: The changes of the head group order parameters of POPC bilayer as a function of NaCl concentrations from simulations with different force fields together with experimental data for DPPC [4] and POPC [5]. Ion concentrations in x-axis are calculated as in Fig. 3. Simulation data with Lipid14 and Åqvist ion parameters is taken directly from Refs. [51, 54].

25.Add also the POPC result to the figure. Ref.[5] gives for POPC at 1M of NaCl

$$\Delta S^\alpha = (6.1 - 5.5) * 0.00784 = 0.004704.$$

26.Add temperatures to the experimental data.

27.Labeling should be consistent with the previous figure, i.e. experimental data with diamonds etc.

28.x-axis scale from -1 to 1100 to make the point in zero fully visible and to remove empty space.

29.Empty space between figures and from the right column could be reduced.

ing the importance of the comparison of the lipid headgroup order parameter response to the bound charge between simulations and experiments as done in section III B.

The ion binding affinity of ECC-lipid model with different water models is compared in SI. The performance with all water models is better than in in the original Lipid14 parameteres, but the order parameter changes are slightly overestimated with all four-site water models and with TIP3P.

D. Affinity and binding cites to POPC membrane

The binding affinities of Ca^{2+} ions to POPC bilayer in different simulation models were quantified by calculating the relative surface excess from Eq. 4 using the bulk concentrations determined from the density profiles in Fig. 5. The relative surface excess values, shown in Table II, were cal-

TABLE II: The relative surface excess and the probabilities of contacts between bound Calcium and different oxygen moieties in POPC from different simulation models. The $CaCl_2$ concentration of the ions in water is 350mM in the analyzed systems.

model	Γ_{Ca}^{w} (nm^{-2})	$P_{PO_4}^{Ca^{2+}}$	$P_{O_{carb.}}^{Ca^{2+}}$
ECC-lipids	0.07 ± 0.01	99%	25%
Lipid14/Åqvist	0.13 ± 0.01	-	-
Lipid14/Dang	0.3 ± 0.03	-	-

culated from simulations with the same, $350\,\mathrm{mM}$, concentration of $CaCl_2$ with respect to water, i.e., the concentration before solvating the lipids in experiments. As expected from the changes of the lipid headgroup order parameters in Fig. 3, the relative surface excess for the ECC-lipid model, $\Gamma_{Ca}^{w} = 0.07 \pm 0.01\mathrm{nm}^{-2}$, is significantly smaller than for the Lipid14 model with Åqvist ions, $\Gamma_{Ca}^{w} = 0.13 \pm 0.01\mathrm{nm}^{-2}$, or with Dang ions, $\Gamma_{Ca}^{w} = 0.3 \pm 0.03\mathrm{nm}^{-2}$. **32.JOE: I'd put the Γ values into a table SAMULI: They are now in the table II together with probabilities of the calcium binding probabilities to different POPC oxygens. However, I am not sure if the table is useful in the end.** Interestingly, the relative surface excess of NaCl at $1\,\mathrm{M}$ concentration (ECC-ions [22]) calculated using density profiles in Fig. **??** is qualitatively different from $CaCl_2$ having a negative value $\Gamma_{i}^{w} = -0.1 \pm 0.01\mathrm{nm}^{-2}$, meaning that water molecules are preferred to sodium and chloride ions at the membrane-water interface. This is in contrast to the most of the available lipid force fields, which predict a specific binding of sodium on PC lipid bilayers [18]. **33.Densities and relative surface excess from NaCl systems to be added. The discussion above to be finished after this.**

The probabilities for a bound Ca^{2+} ion to interact with different oxygen moieties of POPC were analyzed by counting the contacts within the distance of $0.3\,\mathrm{nm}$, as done previously in Ref. 14. The results in Table II show that almost all (99%) of the bound Ca^{2+} ions are in contact with the phosphate oxygens and a quarter of them (25%) interacts with the carbonyl oxygens. Thus, the interactions between Calcium ions with only carbonyl oxygens are very unlikely (1%), but significant amount of the ions interact with both, phosphate and carbonyl oxygens. The individual lipids or acyl chains were not identified in the analysis, thus the simultaneous ion contacts with both oxygen moieties may be inter or intra molecular and occur with the carbonyls in the either of the acyl chains. The most likely contacts between Ca^{2+} ions and phosphate oxygens is visualized with the probability isodensity contours in Fig. 6. While the higher concentrations of $CaCl_2$ naturally increased the amount of contacts per lipid, the distribution of contacts between phosphate and carbonyl oxygens was not affected.

Even thought Na^+ ions bind to POPC bilayer with a very low probability, it was possible to analyze the distribution of contacts from simulations with a large sodium concetration of 1 M. The results show that Na^+ ions bind only to the phosphate oxygens of POPC with the probablity of 55% and only to the carbonyl oxygens with the probability of 20%, leaving the probability of 25% for the simultaneous binding to both.

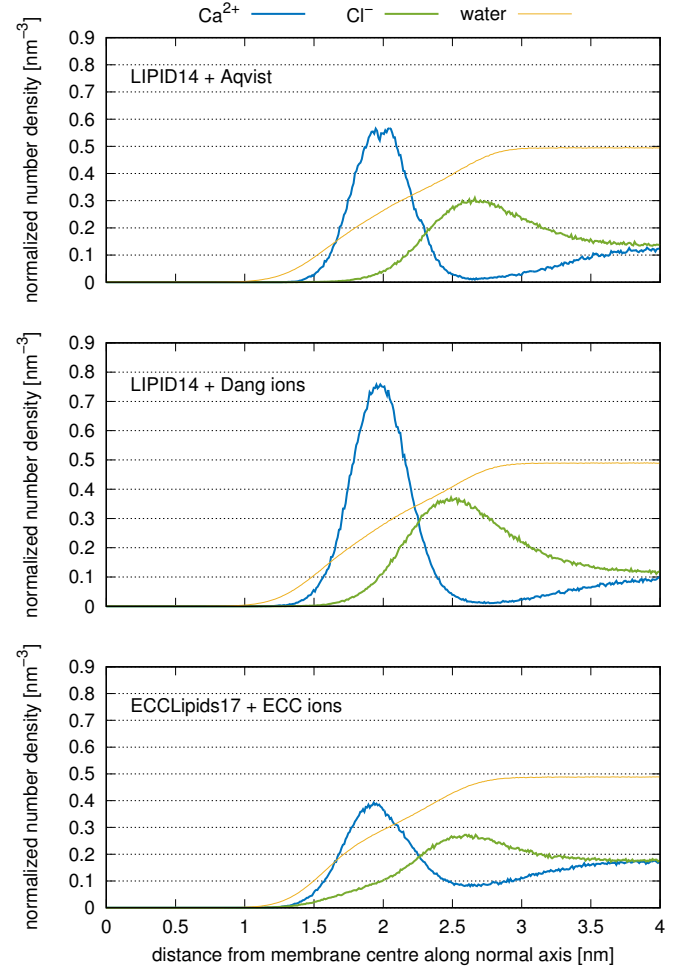In conclusion, the results suggest that the Calcium ions

FIG. 5: Number density of Ca^{2+} and Cl^- as a function of membrane normal axis for different force fields. Data for Lipid14 with Åqvist ions are taken directly from Ref. 18. Densities of Cl^- and water are divided with 2 and 200, respectively, to visalize them with the same scale as Ca^{2+}. The molar concentration of the ions in water is 350 mM in all systems presented here.

34.PAVEL: draw phosphate position with its variance, add water density (scaled) and include the number of Γ-surface access.

35.JOE: Change the figure so that it contains a membrane background

specifically bind to phosphate oxygens, while occasionally interacting also with carbonyls. This is in good agreement with the previous conclusions from several experimental and theoretical studies [3, 7, 15–17], but suggests lower relative binding affinity to carbonyls than the previous MD simulation studies [10, 11, 13, 14]. Also the Sodium ions bind most likely to the phosphate oxygens, while the probability of binding purely to carbonyls is also significant, in contrast to Calcium ions. The physiological relevance of the Sodium binding details is, however, uncertain due to the very weak binding affinity.
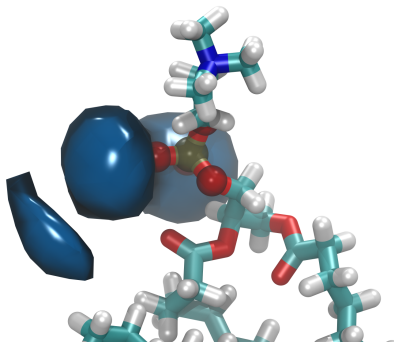
FIG. 6: Contours of probability isodensities of Ca^{2+} with respect to the phosphate oxygens of POPC from ECC-lipid simulation.

E.   Binding stoichiometry to POPC membrane

Simple binding models have been previous used to interpreted the same experimental data, which is used in this work to validate the simulation models in Fig. 3 [5, 69]. The experimental results from the lipid headgroup order parameters and from the atomic absorption spectroscopy were best explained by the ternary complex binding model with a binding stoichiometry of one Ca^{2+} per two POPC lipids [5]. However, also a Langmuir adsorption model (i.e. Ca^{2+}:POPC stoichiometry of 1:1) was successfully fit to the experimental data when only low concentrations of $CaCl_2$ were considered [69]. The results based on these binding models and the measured headgroup order parameter changes are also inluded in the tabulated experimental binding constants [70].

Since the same experimental data is reproduced by the ECC-lipid model, it can be used to give a more versatile interepration of the binding stoichiometry than the previously used simple binding models [5, 69]. To directly evaluate the stoichiometry from simulations we calculated the relative propensities of Ca^{2+}:POPC complexes with various stoichiometries by counting the individual lipid molecules within the distance of $0.3\,nm$ from each Ca^{2+} ion. The results from POPC simulation with 285 mM concetration of $CaCl_2$ in Fig. 7 show the largest propensity (42%) for the ternary complex with the Ca^{2+}:POPC stoichiometry of 1:2, but the probabilities for the complexes with the stoichimetries of 1:1 (30%) and 1:3 (28%) are only slightly lower, suggesting more complex binding stoichiometry than the simple ternary complex model. However, one Calcium binds roughly to two lipids on average also in simulations, because the probabilities of forming the complexes with 1 or 3 lipids are almost equal. This probably explains the successfull fit of the ternary complex model to the experimental data. Complexes with more than three lipids per one Calcium ion were not observed in simulations with the ECC-lipids model. **37.I think that we either have to do the analysis in SI properly, i.e., using the real C_I from simulations or remove the sentence below and the related concent from SI.** Ternary complex model also provides a good fit to our simulations with ECC-
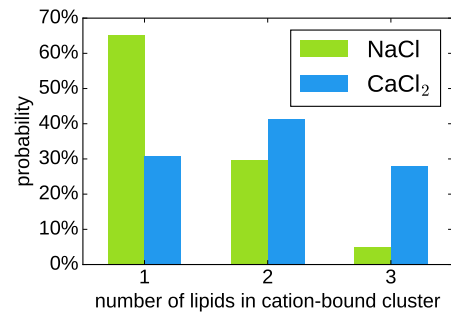
FIG. 7: Relative probabilities of existence of Na^+ or Ca^{2+} complexes with a certain number of POPC lipids. Na^+ complexes were evaluated from the simulation with 1 M concentration; and Ca^{2+} complexes were evaluated from the simulation with 287 mM concentration.

lipids (see Fig. 8 in SI and its caption for details).

Also the probabilities of different complexes formed by Na^+ ions and POPC analyzed from the ECC-lipid model simulation with 1 M concentration of NaCl are shown in Fig. 7. In contrast to Calcium, the probability is largest (??%) for 1:1 complex, significantly smaller (??%) for 1:2 complexes and very small (??%) for 1:3 of Na^+:POPC complexes. **38.Add numbers for Sodium.**

F.   Residence times of Na^+ and Ca^{2+} cations in POPC membrane

Equilibration of Ca^{2+} binding to POPC bilayer takes hundreds of nanoseconds in MD simulations with CHARMM36 and Slipids force fields [14], suggesting that simulations with the length of several microseconds would be required to study the binding phenomena in equilibrium. However, the density profiles of Ca^{2+} from the ECC-lipid simulation in Fig. 5 show a relatively shallow minimum at the interface, suggesting a smaller barrier for the exchange of Calcium ions. To quantify the ion binding exchange in lipid bilayer simulations, we calculated the residence times of ions within the distance of 0.3 nm from any oxygen atom belonging to a lipid molecule in a bilayer.

The residence time histograms of Ca^{2+} in POPC bilayer are shown in Fig. S**??** in SI from the ECC-lipid simulation with $CaCl_2$ concentration of 1 M and from the CHARMM36 simulation with 450 mM concentration of ECC-ions taken from the previous study [14] (the simulation data was downloaded from Ref. 71). **39.JOE: Plot a histogram of residence times based on our simulations and simulation from 14 and put it into SI. 40.It might be also better to do the analysis from ECC-lipid simulation with concentration closer to the data in literature, i.e. 450mM.** Approximately 20% of the Ca^{2+} residence times in the CHARMM36 simulation are longer than the lenght of the trajectory (800 ns), and only less than 60% of the bound residence times are shorter than the half of the simulation length (400 ns). Even longer residence times are observed in the other simulations with CHARMM36 and Slipids models reported in the previous work [14]. At least order of mag-

nitude faster exchange is observed in the ECC-lipid model, where 90% of the Ca^{2+} residence times to a POPC membrane are shorter than 60 ns, and the longest observed residence time in the ECC-lipid simulation is 120 ns, which is well below the total length of the simulation (200 ns). The exchange of Na$^+$ ions to a POPC membrane is an order of magnitude faster, giving 90% of the residence times smaller than 2 ns, the longest residence time being 13 ns. All the results are in line with the experimental estimation that the residence time of Ca^{2+} at the individual PC headgroup is shorter than 10 μs [5].

In conclusion, the results from ECC-lipid model suggest that the exchange of bound Calcium occurs within ∼100ns timeframe, which is much faster than previously reported [14]. The sodium exhibit even faster exchange. This suggests that simulations with the length of few hundred nanoseconds are sufficient to simulate equilibrium ion binding to PC lipid bilayers, when realistic force fields are used. This has not been the case with the available lipid force fields, which overestimate the binding streght of the cations [14, 18].

1. Internal side-note:

However, $\Sigma_{\mathrm{O_{carb.}}}^{\mathrm{Ca^{2+}}}$ is increased in simulation withy the highest CaCl$_2$ concentration when carbonyl dipoles are scaled only with 0.945 (roughly done through charge redistribution) to : $\Sigma_{\mathrm{O_{carb.}}}^{\mathrm{Ca^{2+}}} \approx 0.08$.

The average number of contacts per lipid between Ca^{2+} and any oxygen atom in POPC is $\Sigma_{\mathrm{O}}^{\mathrm{Ca^{2+}}} = 0.264 \rightarrow 0.309$, whereas if only phosphate oxygen atoms are considered the average number of contacts decreases only by a tiny amount to $\Sigma_{\mathrm{PO_4}}^{\mathrm{Ca^{2+}}} = 0.262 \rightarrow 0.303$, and if only carbonyl oxygen atoms are considered (phosphate oxygens contribute, but are not counted as contacts), this value is merely $\Sigma_{\mathrm{O_{carb.}}}^{\mathrm{Ca^{2+}}} = 0.066 \rightarrow 0.139$.

This means that calcium is in contact with a phosphate oxygen for 98% of the time it is bound to the membrane, whereas 46% of the time accounts for contact with a carbonyl oxygen, and purely carbonyl bound states account for less than 2% of configurations. The states that have a contribution from carbonyl oxygens also contain a bound phosphate, so it can be thought of rather as a stabilizing moiety.

The residence times change to 75ns (90% of bound time) and max is 185ns. That's not much, too. It certainly is not a game changer, I'd even call it to be within accuracy. The slight problem may be that with this tweak, there's approx. 17% more cations bound to the membrane, which means, I'd need to tune the sigma parameter a bit (increase the scaling factor f_σ). That could detune the membrane structure . . . Not f_q – that's set by the simulations with the surfactant. Good. I think that such a binding detail is within the accuracy of the proposed simple correction. It would be worth noting that the model may underestimate slightly the contribution from carbonyls due to this. But we can't say to what extent. . .

IV. CONCLUSIONS

By using the electrometer concept we show that the binding of Na$^+$ and Ca^{2+} ions to a POPC lipid bilayer can be accurately described with the classical MD simulation force field, where the electronic polarization is implicitly included using the electronic continuum correction (ECC) [21]. The proposed ECC-lipids model is a significant improvement over other available lipid models, which all overestimate specific cation binding affinities [18]. While the structural details of a POPC lipid bilayer simulated with the ECC-lipids model agree with experiments with the comparable accuracy to the other state of the art lipid models, it also reproduces the experimental lipid head group order parameter responses to the cationic surfactant, NaCl and CaCl$_2$ concentrations.

The good agreement with experiments enables the atomic resolution interpretation of NMR experiments by using MD simulations. In agreement with previous interpretations of experimental data [7, 15–17], the Ca^{2+} ions mainly interact with phosphate oxygens. However, the stoichiometry of the binding is significantly more complicated than in the previous interpretation of the NMR data based on the ternary complex model, where one calcium binds to two POPC molecules [5]. The complexes of one calcium bound to two lipids are the most probable also in the ECC-lipids model, but the complexes of one or three lipids per one calcium were observed to be almost equally likely. While the success of the ternary compex model is understandable based on the simulation results, a simple binding model cannot detec the complex binding oberved in the simulation.

The improved cation binding behaviour to POPC bilayer pave the way for simulations of complex biochemical systems with correctly described electrostatic interactions in the vicinity of cellular membranes. The ECC-lipids model is build by scaling the partial charges and the LJ-radius of the headgroup, glycerol backbone and carbonyl atoms of the Lipid14 POPC model [25] with the constant factor of 0.8 and 0.89, respectively. While the Lipid14 model is compatible with the AMBER force field family, the compatibility of the ECC-lipids model may be compromised due to the changes in intermolecular interactions of the scaled atoms. On the other hand, a fully consistent ECC-force field should include the correction also in other than lipid molecules, including water. The work toward this direction and the extension to other lipid molecules and force fields is left for the future studies.

This work can be reached as a repository containing all data at `zenodo.org:\dots\dots\dots`.
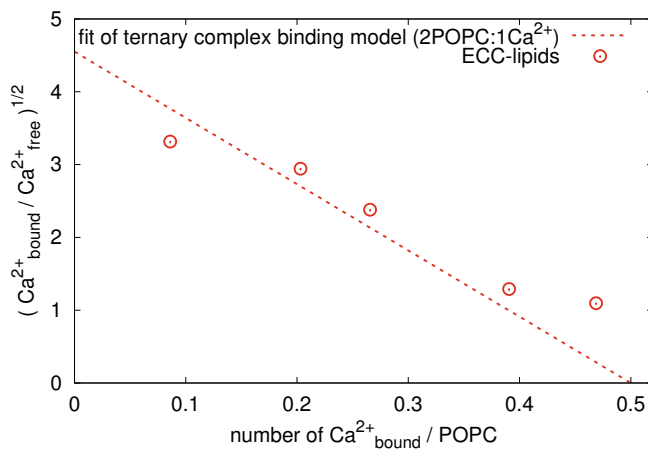
FIG. 8: Ternary complex binding model of Ca^{2+} to a POPC membrane that assumes the stoichiometry of 2 POPC:1 Ca^{2+} (details in reference 5) provides a good fit to experimental measurements [5] and it also provides a good fit to our simulation data. Note that the units in the reference 5 are different from the units presented here, and, hence, the observed slope of the linear relationship is different.

41. This should be either done properly with the correct C_I or removed. Removing might be a better idea at this point. It was found in the original work [5] that a ternary complex binding model (i.e. 2 POPC:1 Ca^{2+}) provides the best fit to experimental measurements of all considered models in that study. In such a model, there is a linear relationship between quantities C_b, mole fraction of bound Ca^{2+} per POPC, and $\sqrt{C_b/C_I}$, where C_I is the concentration of free cations at the plane of ion binding [5]. The concentration C_b was obtained from an extrapolation of linear relation between deuterium NMR measurements and atomic absorption spectroscopy for low concetrations of $CaCl_2$. Such an extrapolation is valid as long as the mode of Ca^{2+} binding remains constant throughout the extrapolation range. The concentration C_I is determined by using the surface potential by using the Boltzmann equation. However, Boltzmann theory yields inaccurate results for divalent cations like Ca^{2+} [72]. An atomistic simulation, on the other hand, provides these quantities directly without severe assumptions. Hence we hypothesise that the discrepancy between the results in the experiment [5] and our simulations likely lays in the fact that the assumptions and relations used for determinig concentrations C_b and C_I in the experiment [5] gradually do not hold for higher concentrations of Ca^{2+}.

SUPPLEMENTARY INFORMATION

[1] P. Scherer and J. Seelig, The EMBO journal **6** (1987).
[2] J. Seelig, Cell Biol. Int. Rep. **14**, 353 (1990), URL http://dx.doi.org/10.1016/0309-1651(90)91204-H.
[3] G. Cevc, Biochim. Biophys. Acta - Rev. Biomemb. **1031**, 311 (1990).
[4] H. Akutsu and J. Seelig, Biochemistry **20**, 7366 (1981).
[5] C. Altenbach and J. Seelig, Biochemistry **23**, 3913 (1984).
[6] J.-F. Tocanne and J. Teissié, Biochim. Biophys. Acta - Reviews on Biomembranes **1031**, 111 (1990).
[7] H. Binder and O. Zschörnig, Chem. Phys. Lipids **115**, 39 (2002).
[8] G. Pabst, A. Hodzic, J. Strancar, S. Danner, M. Rappolt, and P. Laggner, Biophys. J. **93**, 2688 (2007).
[9] D. Uhrkov, N. Kuerka, J. Teixeira, V. Gordeliy, and P. Balgav, Chemistry and Physics of Lipids **155**, 80 (2008).
[10] R. A. Böckmann, A. Hac, T. Heimburg, and H. Grubmüller, Biophys. J. **85**, 1647 (2003).
[11] R. A. Böckmann and H. Grubmüller, Ang. Chem. Int. Ed. **43**, 1021 (2004).
[12] M. L. Berkowitz and R. Vacha, Acc. Chem. Res. **45**, 74 (2012).
[13] A. Melcrov, S. Pokorna, S. Pullanchery, M. Kohagen, P. Jurkiewicz, M. Hof, P. Jungwirth, P. S. Cremer, and L. Cwiklik, Sci. Reports **6**, 38035 (2016).
[14] M. Javanainen, A. Melcrova, A. Magarkar, P. Jurkiewicz, M. Hof, P. Jungwirth, and H. Martinez-Seara, Chem. Commun. **53**, 5380 (2017), URL http://dx.doi.org/10.1039/C7CC02208E.
[15] H. Hauser, M. C. Phillips, B. Levine, and R. Williams, Nature **261**, 390 (1976).
[16] H. Hauser, W. Guyer, B. Levine, P. Skrabal, and R. Williams, Biochim. Biophys. Acta - Biomembranes **508**, 450 (1978), ISSN 0005-2736, URL http://www.sciencedirect.com/science/article/pii/0005273678900913.
[17] L. Herbette, C. Napolitano, and R. McDaniel, Biophys. J. **46**, 677 (1984).
[18] A. Catte, M. Girych, M. Javanainen, C. Loison, J. Melcr, M. S. Miettinen, L. Monticelli, J. Maatta, V. S. Oganesyan, O. H. S. Ollila, et al., Phys. Chem. Chem. Phys. **18** (2016).
[19] R. Vacha, S. W. I. Siu, M. Petrov, R. A. Böckmann, J. Barucha-Kraszewska, P. Jurkiewicz, M. Hof, M. L. Berkowitz, and P. Jungwirth, J. Phys. Chem. A **113**, 7235 (2009).
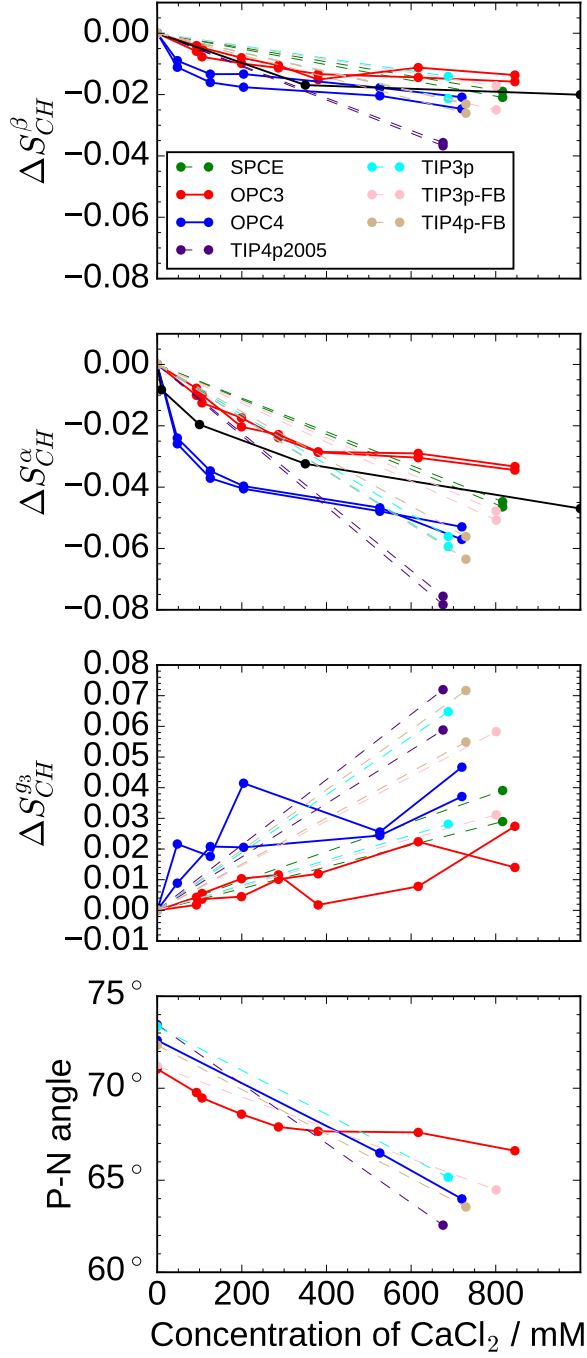[20] J. Seelig, P. M. MacDonald, and P. G. Scherer, Biochemistry

TABLE III: Area per lipid (APL) from different models of POPC with no ions

model	APL ($Å^2$)	Temperature [K]
Lipid14	65.1± 0.6	300
Lipid14 [25]	65.6± 0.5	303
ECC-lipids		
OPC3	62.2± 0.6	300
OPC3	64.2± 0.6	313
SPC/E	65.1± 0.6	313
OPC	64.4± 0.6	313
TIP4p/2005	66.8± 0.6	313
experiment	62.7	293
experiment [39]	64.3	303
experiment	67.3	323
experiment	68.1	333

42. Result with normal TIP3P missing?

FIG. 9: Changes of head group order parameters of POPC bilayer as a function of $CaCl_2$ concentrations are shown from simulations with different force fields and water models together with experimental data (DPPC [4] and POPC [5]). Ion concentrations in bulk water are shown in x-axis. Values from simulations are calculated from the of cation number density C_{np} from the region at the simulatin box edge with the constant ion concentration as [ion]=$C_{np}/0.602$.
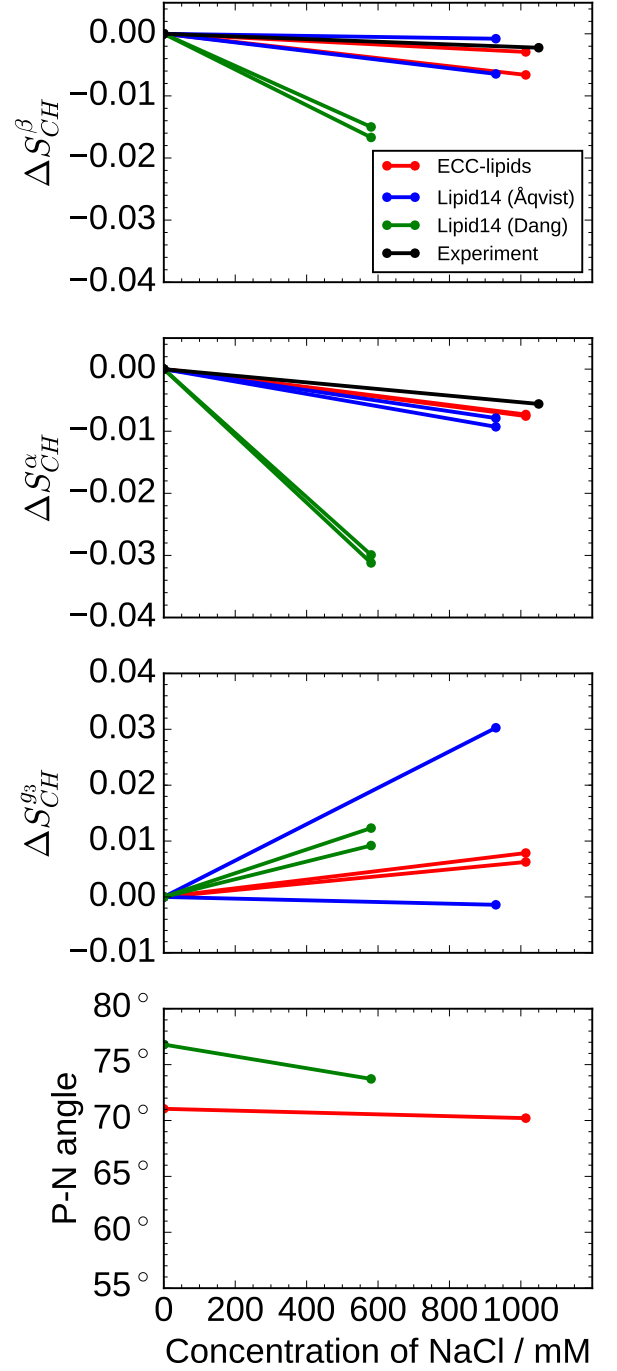
FIG. 10: Changes of head group order parameters of POPC bilayer as a function of NaCl concentrations are shown from simulations with different force fields together with experimental data [4]. Ion concentrations in bulk water are shown in x-axis. Values from simulations are calculated from the of cation number density C_{np} from the region at the simulatin box edge with the constant ion concentration as [ion]=$C_{np}/0.602$. Simulation data with Lipid14 and Åqvist ion parameters is taken directly from Ref. [18].

TABLE IV: Simulation parameters

simulation property	parameter
time-step	2 fs
equilibration time	100 ns
total simulation time	300 ns
temperature	313 K
thermostat	v-rescale [73]
barostat	Parrinello-Rahman, semi-isotropic [74]
long-range electrostatics	PME [75]
cut-off scheme	Verlet [76]
Coulomb and VdW cut-off	1.0 nm
constraints	LINCS, only hydrogen atoms [77]
constraints for water	SETTLE [78]

26, 7535 (1987).

[21] I. Leontyev and A. Stuchebrukhov, Phys. Chem. Chem. Phys. **13**, 2613 (2011).

[22] E. Pluhaová, H. E. Fischer, P. E. Mason, and P. Jungwirth, Molecular Physics **112**, 1230 (2014), ISSN 0026-8976, URL http://www.tandfonline.com/doi/abs/10.1080/00268976.2013.875231.

[23] M. Kohagen, P. E. Mason, and P. Jungwirth, J. Phys. Chem. B **118**, 7902 (2014).

[24] M. Kohagen, P. E. Mason, and P. Jungwirth, J. Phys. Chem. B **120**, 1454 (2016).

[25] C. J. Dickson, B. D. Madej, . A. Skjevik, R. M. Betz, K. Teigen, I. R. Gould, and R. C. Walker, J. Chem. Theory Comput. **10**, 865 (2014).

[26] T. R. Lucas, B. A. Bauer, and S. Patel, Biochimica et Biophysica Acta (BBA) - Biomembranes **1818**, 318 (2012), membrane protein structure and function.

[27] J. Chowdhary, E. Harder, P. E. M. Lopes, L. Huang, A. D. MacKerell, and B. Roux, J. Phys. Chem. B **117**, 9142 (2013).

[28] B. Jonsson, O. Edholm, and O. Teleman, J. Chem. Phys. **85**, 2259 (1986).

[29] E. Egberts, S.-J. Marrink, and H. J. C. Berendsen, European Biophysics Journal **22**, 423 (1994).

[30] I. V. Leontyev and A. A. Stuchebrukhov, The Journal of chemical physics **130**, 085102 (2009), ISSN 1089-7690, URL http://scitation.aip.org/content/aip/journal/jcp/130/8/10.1063/1.3060164.

[31] I. V. Leontyev and A. A. Stuchebrukhov, Journal of Chemical Theory and Computation **6**, 1498 (2010), ISSN 1549-9618, URL http://dx.doi.org/10.1021/ct9005807.

[32] H. Hu, Z. Lu, and and Weitao Yang*, Journal of Chemical Theory and Computation **3**, 1004 (2007), ISSN 1549-9618, URL http://dx.doi.org/10.1021/ct600295n.

[33] C. C. I. Bayly, P. Cieplak, W. D. Cornell, and P. a. Kollman, The Journal of Physical ... **97**, 10269 (1993), ISSN 0022-3654, 93/2091- 10269$04.00/0, URL http://pubs.acs.org/doi/abs/10.1021/j100142a004.

[34] U. C. Singh and P. A. Kollman, Journal of Computational Chemistry **5**, 129 (1984), ISSN 1096987X.

[35] P. G. Scherer and J. Seelig, Biochemistry **28**, 7720 (1989).

[36] O. H. S. Ollila and M. Retegan, *Md simulation trajectory and related files for popc bilayer (lipid14, gromacs 4.5)* (2014), URL http://dx.doi.org/10.5281/zenodo.12767.

[37] A. Botan, F. Favela-Rosales, P. F. J. Fuchs, M. Javanainen, M. Kanduč, W. Kulig, A. Lamberg, C. Loison, A. Lyubartsev, M. S. Miettinen, et al., J. Phys. Chem. B **119**, 15075 (2015).

[38] O. S. Ollila and G. Pabst, *Atomistic resolution structure and dynamics of lipid bilayers in simulations and experiments* (2016), in Press, URL http://dx.doi.org/10.1016/j.bbamem.2016.01.019.

[39] N. Kučerka, M. P. Nieh, and J. Katsaras, Biochim. Biophys. Acta **1808**, 2761 (2011), ISSN 0006-3002.

[40] T. M. Ferreira, R. Sood, R. Bärenwald, G. Carlström, D. Topgaard, K. Saalwächter, P. K. J. Kinnunen, and O. H. S. Ollila, Langmuir **32**, 6524 (2016).

[41] A. Seelig and J. Seelig, Biochemistry **16**, 45 (1977).

[42] J. H. Davis, Biochim. Biophys. Acta - Reviews on Biomembranes **737**, 117 (1983).

[43] G. Beschiaschvili and J. Seelig, Biochim. Biophys. Acta - Biomembranes **1061**, 78 (1991).

[44] D. K. Chattoraj and K. S. Birdi, *Adsorption at the Liquid Interface from the Multicomponent Solution* (Springer US, Boston, MA, 1984), pp. 83–131, ISBN 978-1-4615-8333-2, URL https://doi.org/10.1007/978-1-4615-8333-2_4.

[45] H. J. C. Berendsen, J. R. Grigera, and T. P. Straatsma, Journal of Physical Chemistry **91**, 6269 (1987), ISSN 0022-3654, URL http://links.isiglobalnet2.com/gateway/Gateway.cgi?GWVersion=2{\&}SrcAuth=mekentosj{\&}SrcApp=Papers{\&}DestLinkType=FullRecord{\&}DestApp=WOS{\&}KeyUT=A1987K994100038{\%}5Cnpapers2://publication/uuid/17978EF7-93C9-4CB5-89B3-086E5D2B9169{\%}5Cnhttp://pubs.acs.org/doi/pdf/10.1021/.

[46] D. E. Smith and L. X. Dang, J. Chem. Phys **100** (1994).

[47] T.-M. Chang and L. X. Dang, J. Phys. Chem. B **103**, 4714 (1999), ISSN 1520-6106, URL http://dx.doi.org/10.1021/jp982079o.

[48] L. X. Dang, G. K. Schenter, V.-A. Glezakou, and J. L. Fulton, J. Phys. Chem. B **110**, 23644 (2006), ISSN 1520-6106, URL http://dx.doi.org/10.1021/jp064661f.

[49] J. Aqvist, The Journal of Physical Chemistry **94**, 8021 (1990), URL http://dx.doi.org/10.1021/j100384a009.

[50] W. L. Jorgensen, J. Chandrasekhar, J. D. Madura, R. W. Impey, and M. L. Klein, J. Chem. Phys **79** (1983).

[51] M. Girych and O. H. S. Ollila, *Popc_amber_lipid14_verlet* (2015), URL http://dx.doi.org/10.5281/zenodo.30898.

[52] M. Girych and O. H. S. Ollila, *Popc_amber_lipid14_cacl2_035mol* (2015), URL http://dx.doi.org/10.5281/zenodo.34415.

[53] M. Girych and S. Ollila, *Popc_amber_lipid14_cacl2_035mol* (2016), URL https://doi.org/10.5281/zenodo.46234.

[54] M. Girych and O. H. S. Ollila, *Popc_amber_lipid14_nacl_1mol* (2015), URL http://dx.doi.org/10.5281/zenodo.30865.

[55] M. J. Abraham, T. Murtola, R. Schulz, S. Páll, J. C. Smith, B. Hess, and E. Lindah, SoftwareX **1-2**, 19 (2015), ISSN 23527110, URL http://www.sciencedirect.com/science/article/pii/S2352711015000059.

[56] A. K. Malde, L. Zuo, M. Breeze, M. Stroet, D. Poger, P. C. Nair, C. Oostenbrink, and A. E. Mark, Journal of Chemical Theory and Computation **7**, 4026 (2011).

[57] D. Case, D. Cerutti, T. Cheatham, III, T. Darden, R. Duke, T. Giese, H. Gohlke, A. Goetz, D. Greene, et al., *AMBER 2017*

(2017), university of California, San Francisco.

[58] A. W. SOUSA DA SILVA and W. F. VRANKEN, *ACPYPE - AnteChamber PYthon Parser interfacE.* (2017), manuscript submitted.

[59] O. H. S. Ollila, *POPC bilayer simulated at T313K with the Lipid14 model using Gromacs* (2017), URL https://doi.org/10.5281/zenodo.1020709.

[60] O. H. S. Ollila, *POPC bilayer with 10% of dihexadecyldimethylammonium simulated at T313K with the Lipid14 model using Gromacs* (2017), URL https://doi.org/10.5281/zenodo.1020240.

[61] O. H. S. Ollila, *POPC bilayer with 20% of dihexadecyldimethylammonium simulated at T313K with the Lipid14 model using Gromacs* (2017), URL https://doi.org/10.5281/zenodo.1020593.

[62] O. H. S. Ollila, *POPC bilayer with 30% of dihexadecyldimethylammonium simulated at T313K with the Lipid14 model using Gromacs* (2017), URL https://doi.org/10.5281/zenodo.1020623.

[63] O. H. S. Ollila, *POPC bilayer with 42% of dihexadecyldimethylammonium simulated at T313K with the Lipid14 model using Gromacs* (2017), URL https://doi.org/10.5281/zenodo.1020671.

[64] O. H. S. Ollila, *POPC bilayer with 50% of dihexadecyldimethylammonium simulated at T313K with the Lipid14 model using Gromacs* (2017), URL https://doi.org/10.5281/zenodo.1020689.

[65] T. M. Ferreira, F. Coreta-Gomes, O. H. S. Ollila, M. J. Moreno, W. L. C. Vaz, and D. Topgaard, Phys. Chem. Chem. Phys. **15**, 1976 (2013).

[66] A. Seelig and J. Seelig, Biochim. Biophys. Acta **406**, 1 (1975).

[67] H. Schindler and J. Seelig, Biochemistry **14**, 2283 (1975).

[68] K. Gawrisch, D. Ruston, J. Zimmerberg, V. Parsegian, R. Rand, and N. Fuller, Biophys. J. **61**, 1213 (1992).

[69] P. M. Macdonald and J. Seelig, Biochemistry **26**, 1231 (1987).

[70] D. Marsh, *Handbook of Lipid Bilayers, Second Edition* (RSC press, 2013).

[71] M. Javanainen, *POPC with varying amounts of cholesterol, 450 mM of CaCl_2. Charmm36 with ECC-scaled ions* (2017), URL https://doi.org/10.5281/zenodo.259376.

[72] D. Andelman, in *Handbook of biological physics* (Elsevier Science, 1995), vol. 1, chap. 12, pp. 603–642, URL http://hwiki.liebel-lab.org/wiki/images/9/90/AndelmannReview.pdf.

[73] G. Bussi, D. Donadio, and M. Parrinello, J. Chem. Phys **126** (2007).

[74] M. Parrinello and A. Rahman, J. Appl. Phys. **52**, 7182 (1981).

[75] T. Darden, D. York, and L. Pedersen, J. Chem. Phys **98** (1993).

[76] S. Páll and B. Hess, Computer Physics Communications **184**, 2641 (2013), ISSN 0010-4655, URL http://www.sciencedirect.com/science/article/pii/S0010465513001975.

[77] B. Hess, H. Bekker, H. J. C. Berendsen, and J. G. E. M. Fraaije, J. Comput. Chem. **18**, 1463 (1997).

[78] S. Miyamoto and P. A. Kollman, J. Comput. Chem **13**, 952 (1992).

ToDo

P.